ELSEVIER

Journal of Chromatography A, 716 (1995) 35–48

JOURNAL OF CHROMATOGRAPHY A

Some practical aspects of utilizing the on-line combination of isotachophoresis and capillary zone electrophoresis

Ludmila Křivánková, Petr Gebauer, Petr Boček*

Institute of Analytical Chemistry, Academy of Sciences of the Czech Republic, CZ-611 42 Brno, Czech Republic

Abstract

The on-line combination of isotachophoresis (ITP) and zone electrophoresis is a very effective tool for increasing the separation capability and sensitivity of capillary zone electrophoresis (CZE). Its most effective version is performed in column coupling instrumentation and is characterized by isotachophoresis in the first capillary serving as the efficient preseparation and concentration stage followed by on-line transfer of the sample cut into the second capillary where analytical zone electrophoresis proceeds as the second stage. The on-line transfer of the sample from the first capillary into the second is always accompanied by the segments of some additional amounts of the leader and/or terminator from the ITP step. This results in transient survival of isotachophoretic migration during the second stage. Hence the separation process during the second stage can be characterized as the destacking of analytes followed by zone electrophoretic separation. In this paper, both a theoretical and an experimental study is presented showing that destacking of analytes is a selective process, which affects strongly the most important final analytical parameters of the detected zones, namely the detection time and zone variance, and thus it makes the simple use of detection data for qualitative analysis misleading. It was shown that both the detection time and variance of a zone of an analyte depend strongly on the amount of the accompanying segments of the leader/terminator transferred and on the actual type of electrolyte system selected from the generally possible types. These types are (i) L–S–L, where the leading electrolyte (L) from ITP stage serves as the background electrolyte (BGE) during CZE (S = sample), (ii) T–S–T, where the terminating electrolyte (T) from the ITP stage serves as the BGE during CZE, and (iii) BGE–S–BGE, where L, T and BGE are mutually different. Explicit equations were derived enabling one to predict migration time and zone variance for actual working conditions, and, for model systems, the theoretical data were calculated and verified experimentally. Further, it is shown that the systems T–S–T and L–S–L are user friendly and a simple standardization procedure was proposed, allowing correct qualitative evaluation of the analytical data in these systems. Finally, a theory is presented predicting the existence of anomalous variances of zones in the record of analysis in BGE–S–BGE systems and its experimental verification is given.

1. Introduction

It has been proved that the on-line combination of isotachophoresis (ITP) and zone electrophoresis is an effective tool for improving the analytical expediency of capillary electrophoresis [1–22]. The concentration capability and reproducible sampling inherent in isotachophoresis are combined here with the high resolving power and high sensitivity of capillary zone electrophoresis (CZE). The concentration capability of ITP and the resolving power of CZE follow from

* Corresponding author.

0021-9673/95/$09.50
SSDI 0021-9673(95)00553-6

the principles of these methods and can be affected mainly by the composition of the electrolyte system used. The reproducibility of the sampling and the sensitivity of the methods are mainly influenced by the construction elements of the instrumentation and the type of detection used [23,24], although the selection of the electrolyte system also has a significant impact [25–28]. Owing to its capability to concentrate trace analytes from large sample volumes, it is always ITP which is used in the first stage of the analysis. Isotachophoretic migration during an electrophoretic analysis can be either arranged by directly implanting an ITP electrolyte system in the background electrolyte (BGE) chosen for CZE [3,6,7,10,13–15,17,19–21] or induced by the composition of the sample containing a major component playing for some time the role of the leading or terminating ion [11,19,27].

By far the most effective system described was that employing the capillary for the ITP separation coupled on-line with the second capillary destined for the CZE run [1,2,4–6,8–10,13, 16,18]. Here, in addition to the concentrating effect, also the load capacity of the preseparation ITP step can be increased by employing the first capillary of wider diameter compared with the second capillary [4,6,13,18]. The detectability can increase by more than 10^3-fold [6,9,13,18] and a detection limit as low as 10^{-9} mol/l has been reported [18]. Bulk to trace sample components in a concentration ratio up to 10^5:1 can be determined simultaneously [1]. While the major component is detected in the ITP step and subsequently driven out of the system to the helping electrode, the minor components in the form of a short stack of sharp zones are driven by voltage into the second capillary where the zone electrophoretic migration occurs.

The timing of the transition of ITP into ZE migration depends on the electrolytes used both in the ITP and CZE step and on the amount of the ITP components transferred into the CZE mode. Here, attention must be paid to the fact that the stack of analytes is sandwiched between other zones migrating isotachophoretically, including small parts of the leading and terminating zones as a residue of the ITP migration mode [4,22]. This influences strongly the results of the analysis, especially the detection times of analytes used for identification of the analytes in CZE separations [28]. From this point of view, three combinations of electrolyte systems can be distinguished having a distinct effect of the ITP transient stage on the resulting course of the separation. Either the leading (L) or the terminating (T) electrolyte from the ITP separation can be used as the BGE, or an electrolyte different from these can be applied. We then speak about T–S–T, L–S–L and BGE–S–BGE electrolyte systems (S = sample), and in each of them, the destacking proceeds differently, which affects the resulting image of the separation. The theory revealed that the sample components leave the transient ITP stack gradually in dependence on their mobilities and therefore each sample component starts its ZE migration at a different time and at a different position along the migration path [22]. Therefore, it is not possible to evaluate detection times from the CZE stage in combined ITP–CZE in the same simple way as is done in the single CZE separation mode. Many operational variables have to be taken into account; however, optimum conditions for the separation can be found and correct qualitative identification is also possible.

The temporal stacking effect influences also the zone dispersion. It was shown [29] for a single-capillary system that as long as a minor sample zone migrates in stack, it keeps its size (zone width, variance) almost constant and comparable to the size of the stacking (sharp) zone boundary. The normal dispersion process starts after the zone is destacked. Sample zones in ITP–CZE systems are thus usually sharper than those in comparable CZE systems because their dispersion is retarded during a part of their migration path.

This work was aimed at continuing the previous research [22] by investigating both theoretically and experimentally the major effects of temporal sample stacking in ITP–CZE systems on the final parameters of a sample zone. Atten-

tion is focussed especially on the qualitative identification of analytes and the efficiency of the separation.

2. Theory

2.1. General remarks

The same simple model as described previously [22] was used. The system is assumed to be closed (with zero electroosmotic flow) and diffusion to be the only dispersion effect present. The scheme of the column coupling part of the system is given in Fig. 1 for both T–S–T and L–S–L arrangements. Panels A show the moment when the current is just switched over across the system of both capillaries and the migration of the segment of ITP zones responsible for the transient stacking (i.e., L for the T–S–T system and T for the L–S–L system) into the analytical capillary starts. The original (ITP) zone stack still survives including the sample zone(s). Panels B show the moment when the migration of the stacking zone segment into the analytical capillary has just stopped. The time count begins ($t = 0$) at the moment when only the BGE is present both in front of and behind the stacking and sample zones. This corresponds to the situation shown in panel A for the T–S–T system and in panel B for the L–S–L system.

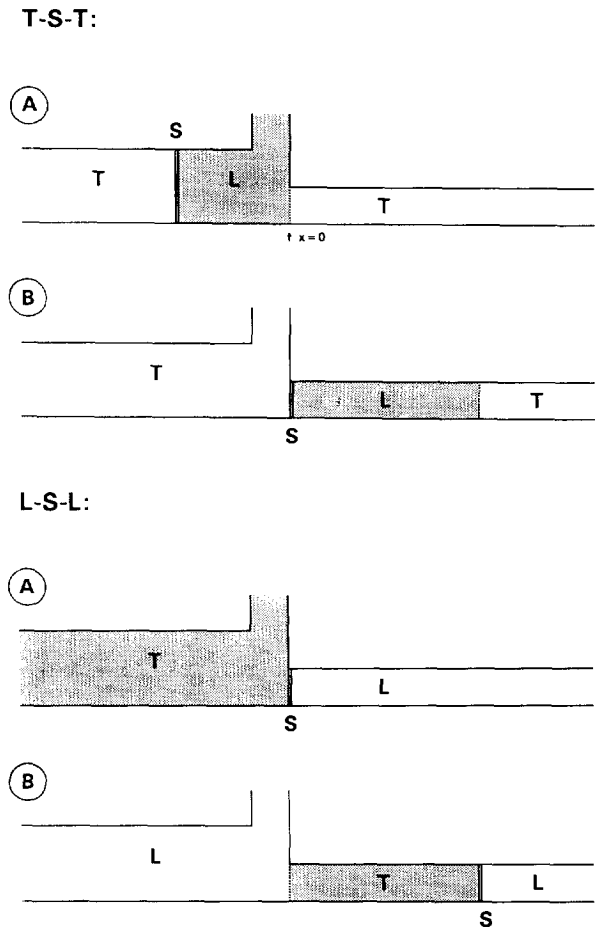

Fig. 1. Scheme of the interface in the column-coupling ITP–CZE arrangement for the T–S–T and L–S–L systems. The preseparation (wide) capillary is located on the left and the analytical (narrow) capillary on the right. The leading, sample and terminating zones are marked as L, S and T, respectively. The arrow shows the origin of the longitudinal coordinate ($x = 0$, positive to the right) used in the calculations. For further explanation, see text.

2.2. Effect of temporal stacking on detection time

In rigorous zone electrophoretic migration, the detection time t_X of an analyte X is the main directly available parameter for the qualitative evaluation of the analysis. It is indirectly proportional to the effective mobility:

$$t_{X,r} = \frac{x\kappa}{i\bar{u}_X} \quad (1)$$

where x is the migration path, $\bar{u}_X$ is the effective mobility of analyte X, κ is the specific conductivity and i is the electric current density (assumed to be constant during the analysis). The simple relationship (1) is not valid, however, in processes where transient ITP migration takes place. The velocity of migration of an analyte differs in the ITP and ZE modes and, as a result, the detection time can be either increased or decreased when compared with the velocity of migration in the ZE mode only. It was shown [22] that the main factors bringing the differences are the magnitude of the segments of the leading zone introduced into the T–S–T system,

the magnitude of the segment of the terminating zone introduced into the L–S–L system and the magnitudes of both of them introduced into the BGE–S–BGE system.

The increase in the detection time of a zone stacked temporarily in a T–S–T system can be expressed by [22]

$$t_{X,r} = \frac{x_r \kappa_T}{i\bar{u}_X} + \frac{u_L - u_T}{u_L - \bar{u}_X} \cdot t_0 \qquad (2)$$

where x_r is the distance of the detector from the inlet of the analytical capillary ($x = 0$), κ_T is the specific conductivity of the background electrolyte (here formed by the terminator from the ITP step) in the analytical capillary, i is the electric current density in the analytical capillary and t_0 is the time of the migration of the leading zone segment into the analytical capillary (i.e., into the ZE stage). This equation can be rewritten in the simple form

$$t_{X,r} = a_1 + b_1 t_0 \qquad (3)$$

where a_1 and b_1 are constants, predicting a linear dependence of $t_{X,r}$ on t_0; Fig. 2 illustrates this, showing a calculated example for three model substances.

Eqs. 2 and 3 hold only for sample zones that had left the stack before they entered the detection cell, i.e. only such $t_{X,r}$ values have physical meaning for which $t_{X,r} > t_{z,r}$, where $t_{z,r}$ is the detection time of the stacking boundary given by [22]

$$t_{z,r} = \frac{\kappa_T}{iu_L}\left(\sqrt{x_r} + \sqrt{x_d} \cdot \frac{u_L - u_T}{u_T}\right)^2 \qquad (4)$$

The coordinate x_d where the original ITP plateau disappears is given by [22,29]

$$x_d = t_0 \cdot \frac{iu_T^2}{\kappa_T(u_L - u_T)} \qquad (5)$$

so that we can obtain $t_{z,r}$ as a function of t_0:

$$t_{z,r} = \left(\sqrt{x_r \cdot \frac{\kappa_T}{iu_L}} + \sqrt{t_0 \cdot \frac{u_L - u_T}{u_L}}\right)^2 \qquad (6)$$

The course of this function is shown in Fig. 2 by the dashed line. Only $t_{x,r}$ values above this line are valid for the correct detection of zones. The

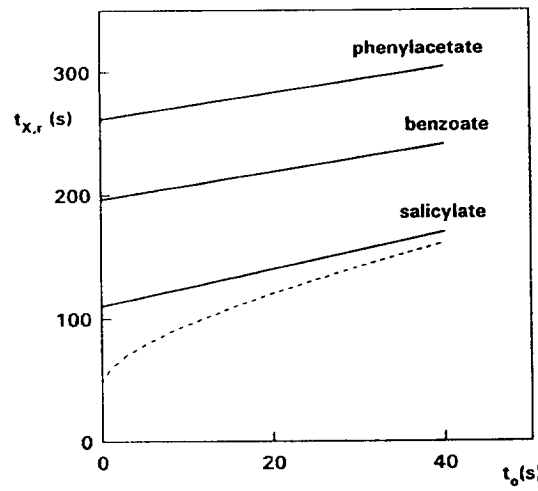

Fig. 2. Calculated dependence of detection time ($t_{X,r}$) of salicylate, benzoate and phenylacetate on the time (t_0) of migration of the leading zone into the analytical capillary in a T–S–T system composed of 0.01 *M* HCl–β-alanine (pH 3.5) (leader) and 0.01 *M* acetic acid–β-alanine (pH 4.3) (terminator, BGE). The effective mobilities of anions used in the calculation were (11.1, 33.3, 18.7 and 14.0)·10^{-9} m^2 V^{-1} s^{-1} for acetate, salicylate, benzoate and phenylacetate, respectively. The calculations were performed for an electric current of 50 μA and a capillary of 300 μm I.D. and 11.5 cm length. For explanation of the dashed curve, see text.

detection times below this dashed line represent the case when transient ITP survived on migrating up to the detection cell. As is seen, for the selected system and three analytes, the danger of being detected still in stack is small here and would require really large segments of the leader being introduced into the ZE stage. This is because the mobilities of all three analytes differ substantially from that of the leading ion.

For the L–S–L system, an equation analogous to Eq. 2 can be derived [22]:

$$t_{X,r} = \frac{x_r \kappa_L}{i\bar{u}_X} - \frac{u_L - u_T}{\bar{u}_X - u_T} \cdot t_0 = a_2 - b_2 t_0 \qquad (7)$$

where $t_0 = l_T \kappa_L / u_L i$ is the time of migration of the segment of the terminating zone into the analytical capillary and l_T is the final length of this zone. Again, a linear dependence of $t_{X,r}$ on t_0 is obtained, with the difference that the slope of the lines is negative, as is shown in Fig. 3 for an example of three model substances. Also here

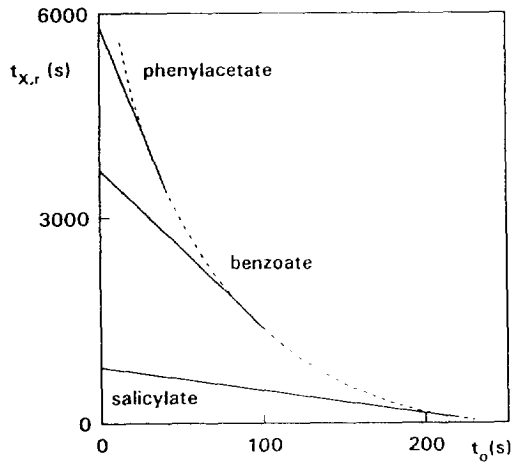

Fig. 3. Calculated dependence of detection time ($t_{X,r}$) of salicylate, benzoate and phenylacetate on the time (t_0) of migration of the terminating zone into the analytical capillary in an L–S–L system composed of 0.01 *M* HCl–β-alanine (pH 3.5) (leader, BGE) and 0.01 *M* acetic acid–β-alanine (pH 4.3) (terminator). The effective mobilities of anions used in the calculation were (25.3, 5.59 and 3.54)·10^{-9} m^2 V^{-1} s^{-1} for salicylate, benzoate and phenylacetate, respectively. The calculations were performed for an electric current of 50 μA and a capillary of I.D. 300 μm I.D. and 11.5 cm length. For explanation of the dashed curve, see text.

the resulting linear dependence of $t_{X,r}$ on t_0 is limited by the condition that the analytes must be out of stack when passing the detector. This can be expressed by $t_{X,r} > t_{z,r}$, where $t_{z,r}$ can be derived from Eq. 16 in Ref. [22]:

$$t_{z,r} = \frac{\kappa_L}{i u_T}\left(\sqrt{x_r} - \sqrt{x_d}\cdot\frac{u_L - u_T}{u_L}\right)^2 \tag{8}$$

By expressing x_d as

$$x_d = t_d u_L \cdot \frac{i}{\kappa_T} = l_T \cdot \frac{u_L}{u_L - u_T} = t_0 \cdot \frac{i}{\kappa_L}\cdot\frac{u_L^2}{u_L - u_T} \tag{9}$$

we can write Eq. 8 as a function

$$t_{z,r} = \left(\sqrt{x_r \cdot \frac{\kappa_L}{i u_T}} + \sqrt{t_0 \cdot \frac{u_L - u_T}{u_T}}\right)^2 \tag{10}$$

In Fig. 3, this function is represented by the dashed curve. The points where the straight lines for actual analytes touch this dashed curve correspond to the limiting case when the analytes reach the detector just being destacked. Only points below the dashed curve have physical meaning and it can be seen that the impact of t_0 on the analytical result is here obviously much more pronounced.

2.3. Effect of temporal stacking on efficiency

It has been shown [29] that the spatial variance in the detection cell, $\sigma^2_{X,r}$, of an electrophoretically migrating sample zone X that has undergone temporal stacking is given by

$$\sigma^2_{X,r} = \sigma^2_{X,e} + 2D_X(t_{X,r} - t_{X,e}) \tag{11}$$

where $\sigma^2_{X,e}$ is the variance of this zone at time $t_{X,e}$ when it leaves the temporal stack and D_X is the diffusion coefficient of the analyte X. When investigating this relationship for the T–S–T system, we can express $t_{X,e}$ on the basis of equations given in Ref. [22] as

$$t_{X,e} = t_0 \cdot \frac{u_L(u_L - u_T)}{(u_L - \bar{u}_X)^2} \tag{12}$$

Using Eq. 12 and assuming that $\sigma^2_{X,e}$ can be neglected, we obtain Eq. 11 in the form

$$\sigma^2_{X,r} = 2D_X\left[\frac{x_r\kappa_T}{i\bar{u}_X} - t_0\cdot\frac{\bar{u}_X(u_L - u_T)}{(u_L - \bar{u}_X)^2}\right] \tag{13}$$

The time-based zone variance can be expressed as

$$\sigma^2_{X,t} = \frac{\sigma^2_{X,r}}{v^2_{X,T}} \tag{14}$$

where $v_{X,T} = \bar{u}_X \cdot i/\kappa_T$ is the zone electrophoretic migration velocity of X in the BGE (here BGE = T). Combining Eqs. 13 and 14, expressing D_X from the Nernst–Einstein equation as RTu_X/F and assuming the sample to be a strong electrolyte ($u_X = \bar{u}_X$), we obtain

$$\sigma^2_{X,t} = \frac{2RT}{F}\left(\frac{\kappa_T}{i}\right)^3\frac{x_r}{\bar{u}_X^2} - 2\cdot\frac{RT}{F}\left(\frac{\kappa_T}{i}\right)^2 \times \frac{(u_L - u_T)t_0}{(u_L - \bar{u}_X)^2} = \frac{a_3}{\bar{u}_X^2} - \frac{b_3 t_0}{(u_L - \bar{u}_X)^2} \tag{15}$$

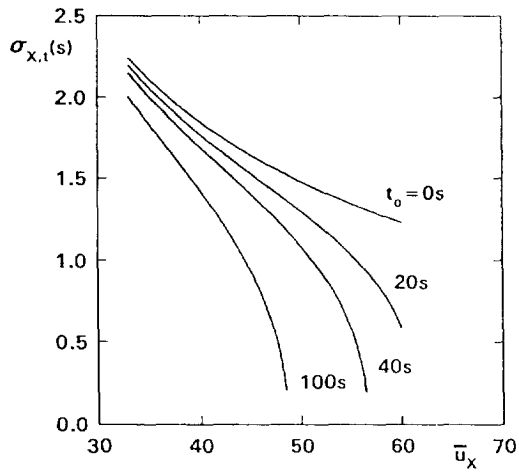

Fig. 4. Calculated dependence of zone width (expressed as time-based standard deviation, $\sigma_{X,t}$) on the effective mobility ($\bar{u}_X$, in 10^{-9} m^2 V^{-1} s^{-1}) of the analyte for various times (t_0) of migration of the leading zone into the analytical capillary in a T–S–T system composed of 0.063 *M* HCl–histidine (pH 6.00) (leader) and 0.045 *M* aspartic acid–histidine (pH 6.15) (terminator, BGE). The calculations were performed for an electric current of 200 μA and a capillary of 300 μm I.D. and 13 cm length.

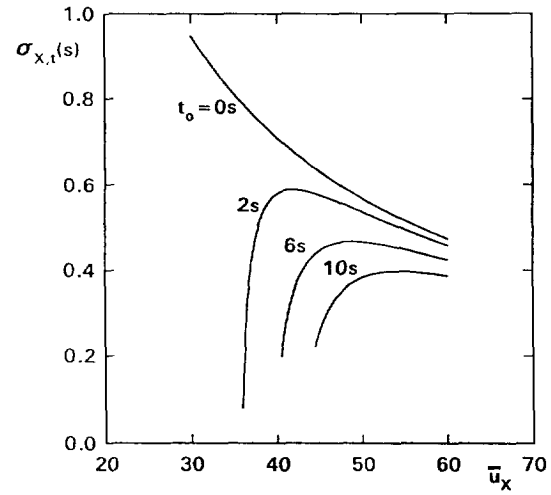

Fig. 5. Calculated dependence of zone width (expressed as time-based standard deviation, $\sigma_{X,t}$) on the effective mobility ($\bar{u}_X$, in 10^{-9} m^2 V^{-1} s^{-1}) of the analyte for various times (t_0) of migration of the terminating zone into the analytical capillary in an L–S–L system composed of 0.01 *M* HCl–histidine (pH 6.00) (leader, BGE) and 0.0071 *M* aspartic acid–histidine (pH 6.15) (terminator). The calculations were performed for an electric current of 150 μA and a capillary of 300 μm I.D. and 13 cm length.

This equation shows the dependence of $\sigma^2_{X,t}$ on $\bar{u}_X$ and on t_0, as is illustrated in Fig. 4 for a given model example (T–S–T system, see captions). The curve for $t_0 = 0$ represents rigorous zone electrophoresis. The larger is t_0 (i.e., the longer the segment of L), the narrower is the mobility region of substances that can reach the detector already destacked (and more dispersed). For a given t_0, the zone dispersion decreases with increasing $\bar{u}_X$ because the more mobile substances remain stacked for a longer time than the less mobile substances.

For the L–S–L system, Eq. 11 is also valid. For substitution of $t_{X,r}$, however, Eq. 7 must be used and for $t_{X,e}$ it can be derived by using Eqs. 9, 11 and 18 in Ref. [22] (with $t_0 = l_L/v_{T-L}$) that

$$t_{X,e} = t_0 \cdot \frac{u_T(u_L - u_T)}{(\bar{u}_X - u_T)^2} \qquad (16)$$

Using a similar procedure as in the previous case, we obtain in analogy

$$\sigma^2_{X,r} = 2D_X\left[\frac{x_r\kappa_L}{i\bar{u}_X} - t_0 \cdot \frac{\bar{u}_X(u_L - u_T)}{(\bar{u}_X - u_T)^2}\right] \qquad (17)$$

$$\sigma^2_{X,t} = \frac{2RT}{F}\left(\frac{\kappa_L}{i}\right)^3 \frac{x_r}{\bar{u}_X^2} - 2 \cdot \frac{RT}{F}\left(\frac{\kappa_L}{i}\right)^2 \times \frac{(u_L - u_T)t_0}{(u_X - \bar{u}_T)^2} = \frac{a_4}{\bar{u}_X^2} - \frac{b_4 t_0}{(u_X - \bar{u}_T)^2} \qquad (18)$$

Fig. 5 illustrates the dependence described by Eq. 18 for an L–S–L model example. The curve for $t_0 = 0$ shows a similar course to that in Fig. 4, but for $t_0 > 0$ the courses are different in principle. The differences are clearly seen for the other curves, which drop abruptly when approaching low $\bar{u}_X$ values. This is explained by the fact that analytes with low mobilities (but not lower than u_T) are stacked for a longer time than those with high mobilities. It should be stressed here that Fig. 5 predicts the existence of stacking-induced zone-variance inversion where the slowest zone is the narrowest and the fastest zone is the widest when passing the detector.

It is interesting to investigate now how the above-described rules for the zone variance demonstrate themselves in a more complicated system such as the BGE–S–BGE system. Here

the segments of the original leading and terminating zones are cut into the ZE stage. Depending on the mobility of the selected BGE, the analyte zones are stacked either by the leading or by the terminating segment and the whole train of transient ITP zones can be considered as consisting of two independent systems. The variance of an analyte zone is thus described either by Eq. 15 or by Eq. 18 modified as follows:

(i) for analytes with $u_{BGE} < \bar{u}_X < u_L$:

$$\sigma^2_{X,t} = \frac{2RT}{F}\left(\frac{\kappa_{BGE}}{i}\right)^3 \frac{x_r}{\bar{u}^2_X} - 2 \cdot \frac{RT}{F} \times \left(\frac{\kappa_{BGE}}{i}\right)^2 \frac{(u_L - u_{BGE})}{(u_L - \bar{u}_X)^2} \cdot t_L \quad (19)$$

(ii) for analytes with $u_T < \bar{u}_X < u_{BGE}$:

$$\sigma^2_{X,t} = \frac{2RT}{F}\left(\frac{\kappa_{BGE}}{i}\right)^3 \frac{x_r}{\bar{u}^2_X} - 2 \cdot \frac{RT}{F} \times \left(\frac{\kappa_{BGE}}{i}\right)^2 \frac{(u_{BGE} - u_T)}{(u_X - \bar{u}_T)^2} \cdot t_T \quad (20)$$

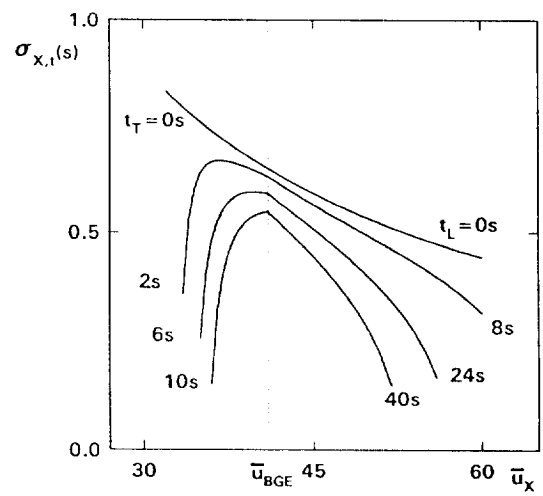

Fig. 6. Calculated dependence of zone width (expressed as time-based standard deviation, $\sigma_{X,t}$) on the effective mobility ($\bar{u}_X$, in 10^{-9} m^2 V^{-1} s^{-1}) of the analyte for various times (t_L and t_T) of migration of the leading and terminating zone, respectively, into the analytical capillary in a BGE–S–BGE system composed of 0.01 *M* HCl–histidine (pH 6.00) (leader), 0.007 *M* aspartic acid–histidine (pH 6.15) (terminator) and 0.01 *M* acetic acid–histidine (pH 6.12) (BGE). The calculations were performed for an electric current of 100 μA and a capillary of 300 μm I.D. and 13 cm length.

where t_L and t_T represent the actual values of t_0 corresponding to the amount of the introduced segments of the L and T zones, respectively. Note that both equations can be used simultaneously for the description of a system, although the starting points for the time count in the zone electrophoretic stage are not the same for cases (i) and (ii); this is because only the difference $t_{X,r} - t_{X,e}$ appears in Eq. 11.

The practical impact of Eqs. 19 and 20 can be again best illustrated by a model example, as shown in Fig. 6. Here, the u_{BGE} value splits the plot into two areas which correspond to the two types of dependence shown in Figs. 4 and 5. In practice this predicts that the zones of analytes of intermediate mobilities (close to the u_{BGE} value) will be the broadest while zones of analytes of both high and low mobilities will be less broad owing to their longer stacking time.

3. Experimental

3.1. Calculations

All calculations were performed for model systems of simplified behaviour. The input ionic mobilities and dissociation constants taken from literature [30] are listed in Table 1. All these values and the effective mobilities of weak acids and bases calculated for a given electrolyte

Table 1
Constants used for the calculations

Substance	Ionic mobility (10^{-9} m^2 V^{-1} s^{-1})	pK_a
β-Alanine	37.5	3.55
Acetate	42.4	4.75
Aspartate	31.6	3.9
Benzoate	33.6	4.2
Chloride	79.1	
H^+	362.5	
Histidine	29.6	6.04
Iodate	42	0.77
Maleate	41; 62.4	1.9; 6.22
Periodate	56.5	1.55
Phenylacetate	31.7	4.4
Salicylate	35.4	3.1

system were assumed to be constant during the analysis.

3.2. Instrumentation

A CS ZKI 01 isotachophoretic analyser (URVJT, Spišská Nová Ves, Czech Republic) equipped with a column-switching system was used. Both preseparation and analytical capillaries were made from PTFE and their I.D. was 0.3 mm. The preseparation capillary was equipped with a conductivity detector positioned 19 cm from the injection point and 5 cm from the bifurcation point. The analytical capillary was equipped with the UV and conductivity detectors placed at distances of 13 cm and 16 cm from the bifurcation point.

The pH of solutions was measured with a Model MS-20 ion activity meter (Laboratorní přístroje, Prague, Czech Republic) with a combined glass electrode.

3.3. Chemicals

Water deionized with a Miele Aqua Purificator G7749 was used for the preparation of both electrolyte systems and sample solutions. All the chemicals used were of analytical-reagent grade and purchased from Lachema (Brno, Czech Republic), except for aspartic acid and histidine, which were from Reanal (Budapest, Hungary).

3.4. Working procedures

The sample was introduced via a sampling valve of 24.5 μl. The first (preseparation) capillary and the corresponding electrode vessels were filled with the isotachophoretic electrolyte system, i.e., with the leading and terminating electrolytes. The second (analytical) capillary and its electrode vessel were filled with the background electrolyte. In the first (ITP) stage, the current passed only through the first capillary between the corresponding electrode vessels containing the leading and terminating electrolyte, respectively. When the rear boundary of the leading zone in the first capillary approached the bifurcation point, the current was switched over to pass through both the preseparation and analytical capillaries.

Suitable timing of this event must be found experimentally with the help of the tell-tale conductivity detector located near the end of the preseparation capillary. Since this detector is placed at a certain distance from the bifurcation block, the exact time when the L–T boundary appears at the bifurcation point must be found by using a suitable dye. This dye is injected as the only analyte into this system, migrates between the leading and terminating electrolyte and is both detected by the tell-tale detector and observed when it reaches the bifurcation point. The time necessary for the boundary to pass the distance between the detector and bifurcation point is constant for constant composition of the leading electrolyte and constant experimental conditions.

Hence the whole train of ionic species in question started to migrate into the analytical capillary. After the whole sample stack entered the analytical capillary, the current was switched off and the terminating electrolyte, now filling the whole preseparation capillary, was washed out and replaced with the BGE. After that the whole separation system was filled with BGE and the stack of sample zones was the only discontinuity in this electrolyte. When the terminator was used as the BGE, the washing step was omitted and the analysis could continue immediately after switching the current over.

The timing of the process is as follows. The time point at which the current is switched over across both capillaries defines the length of the segment of the leading zone entering the analytical capillary expressed in time units. The time of switching the current on after the flushing the terminator out of the preseparation capillary defines the length of the terminating electrolyte that has entered the analytical capillary together with the sample stack. The time counting for the CZE step begins at the moment when the sample being sandwiched by the segments of leading and terminating zones and the whole capillary system being filled with the BGE started to migrate. In the T–S–T system this means that the zone of the sample is still situated in the preseparation

capillary with a segment of leader in front of it, whereas in the L–S–L and BGE–S–BGE systems the sample is already in the analytical capillary followed by the terminator (L–S–L system) or sandwiched by the leader and terminator (BGE–S–BGE system) (see Fig. 1).

4. Results and discussion

The effect of temporal stacking on the detection time is illustrated by Figs. 7 and 8. Fig. 7 is analogous to Fig. 2, showing experimental results in a commonly used ITP buffered electrolyte system (modelling here a T–S–T system) with Cl^- as the leading ion, histidine as the counter ion and aspartate playing here the role of the terminating ion. A 10^{-6} *M* solution of anions of organic and inorganic acids was used as

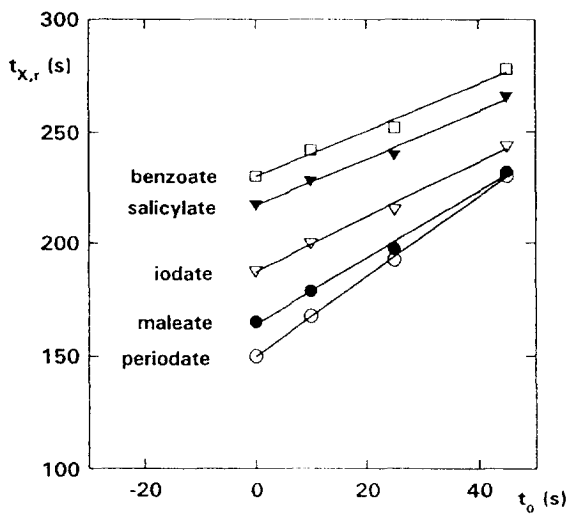

Fig. 7. Experimental verification of the dependence of the detection time ($t_{X,r}$) on the length of the leading zone expressed as the time of its migration into the analytical capillary (t_0) filled with terminator (T–S–T electrolyte system). Measurements were performed at a constant current of 75 μA in both the ITP and CZE migration modes. Leading electrolyte, 10 m*M* HCl–histidine (pH 6.0); terminating electrolyte, 10 m*M* aspartic acid–histidine (pH 6.15). As the background electrolyte for CZE, the terminating electrolyte from the ITP step was used. Sample, 25 μl of $1 \cdot 10^{-6}$ *M* benzoate, salicylate, iodate, maleate and periodate.

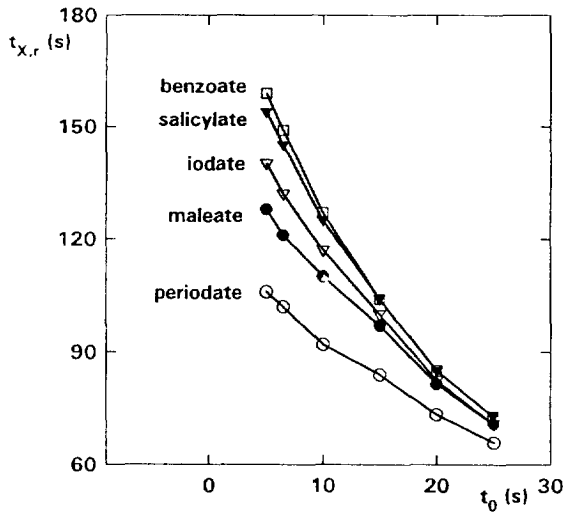

Fig. 8. Experimental verification of the dependence of the detection time ($t_{X,r}$) on the length of the terminating zone expressed as the time of its migration into the analytical capillary (t_0) filled with leading electrolyte (L–S–L electrolyte system). Measurements were performed at a constant current of 75 μA in the ITP mode and 150 μA in the CZE step. Leading electrolyte, 10 m*M* HCl–histidine (pH 6.0); terminating electrolyte, 10 m*M* aspartic acid. As the background electrolyte for CZE, the leading electrolyte from the ITP step was used. Sample, 25 μl of $1 \cdot 10^{-6}$ *M* benzoate, salicylate, iodate, maleate and periodate.

the model mixture. Fig. 7 confirms the linear character of the $t_{X,r}$ vs. t_0 dependence predicted by Eq. 3. It can be seen that the longer the segment of the leading zone that was cut into the analytical capillary, the greater is the prolongation of the detection time. When the segment of the leading zone is very long (i.e., t_0 is high), there is a risk that analytes with the largest mobility can still be migrating in stack when passing the detector (see maleate and periodate at $t_0 = 40$ s).

Such effects (especially for low-mobility analytes) are more pronounced in Fig. 8, showing experimental results based on the same electrolytes as those in Fig. 7 but used in an L–S–L arrangement. The L–S–L system allows one to perform very fast analyses but there is a real danger that if the detector is not placed at a sufficient distance from the bifurcation point, some of the slower analytes can still migrate in

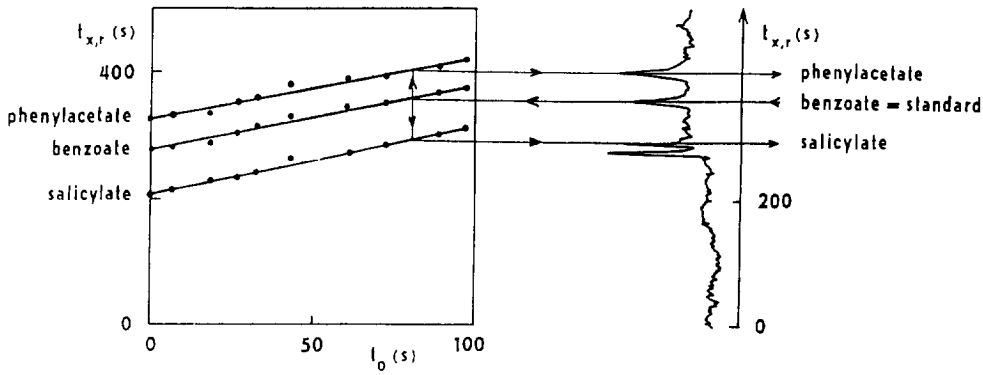

Fig. 9. Principle of the standardization method. To be able to identify analytes in the sample, the calibration graph for the dependence of the detection time of analytes and of an internal standard on the length of the leading electrolyte that had co-migrated with the sample into the CZE step in the case of the T–S–T system (or terminator in the case of the L–S–L system) has to be drawn and used as demonstrated here for the T–S–T system. Measurements were performed at a constant current of 100 μA in the ITP mode and 50 μA in the CZE step. Leading electrolyte, 10 m*M* HCl–β-alanine (pH 3.5); terminating electrolyte, 10 m*M* acetic acid (pH 4.3). As the background electrolyte for CZE, the terminating electrolyte from the ITP step was used. Sample, 25 μl of $1 \cdot 10^{-7}$ *M* salicylate, benzoate and phenylacetate mixture.

stack (see Fig. 8 at higher t_0 values). Also here, the character of the curves fits well with the predictions (see Fig. 3).

Figs. 7 and 8 indicate that the methods (see Ref. [31] and citations therein) utilizing the migration times directly for qualitative evaluation of the analysis may be strongly misleading. Fig. 9 brings a possible solution to this problem, showing the principles of a simple standardization procedure. This procedure requires one to have the experimental dependences of $t_{X,r}$ on t_0 for all analytes of interest and for a selected standard substance. If this standard is added to the analysed sample and it is possible to recognise its peak in the electropherogram of this sample, we can determine the value of t_0 corresponding to the sample and consequently identify the analyte peaks.

The effect of temporal stacking on the efficiency was investigated experimentally first in the most user-friendly T–S–T system. Fig. 10 shows the experimental dependence of time-based peak standard deviation on mobility for a series of weak acids analysed using a BGE composed of 15 m*M* aspartic acid–histidine (pH 6.15). The leader for the ITP step was 10 m*M* HCl–20 m*M* histidine (pH 6). Aspartic acid

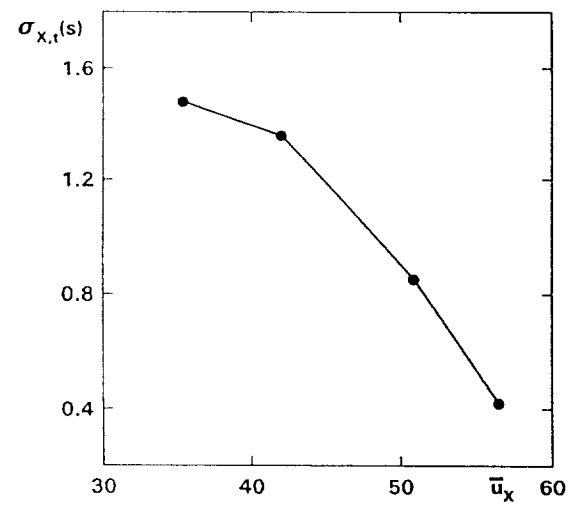

Fig. 10. Experimental verification of the time-based peak standard deviation ($\sigma_{X,t}$) on the mobility of analytes ($\bar{u}_X$, in 10^{-9} m^2 V^{-1} s^{-1}) in the T–S–T system. Measurements were performed at a constant current of 150 μA in both the ITP and CZE modes. Leading electrolyte, 10 m*M* HCl–His (pH 6.0); terminating electrolyte, 15 m*M* aspartic acid–His (pH 6.15). As the background electrolyte for CZE, the terminating electrolyte from the ITP step was used. Length of the leading segment at the beginning of CZE separation, 9 s; sample, 25 μl mixture of $1 \cdot 10^{-6}$ *M* salicylate, iodate, maleate and periodate. The effective mobilities of the analytes at pH 6.00 were calculated from the data given in Table 1.

served as the terminator. Comparison of the results with Fig. 4 demonstrates good coincidence of the experiment with theory, i.e., zone variance in this system decreases with increasing effective mobility.

Fig. 11 presents this dependence for a BGE–S–BGE system composed of 10 m*M* HCl – histidine (pH 6.0) as the leading electrolyte, 10 m*M* aspartic acid as terminator and 10 m*M* acetic acid–histidine (pH 6.12) as BGE. Also here, the comparison with theory is satisfactory and one can see an anomalous course of the

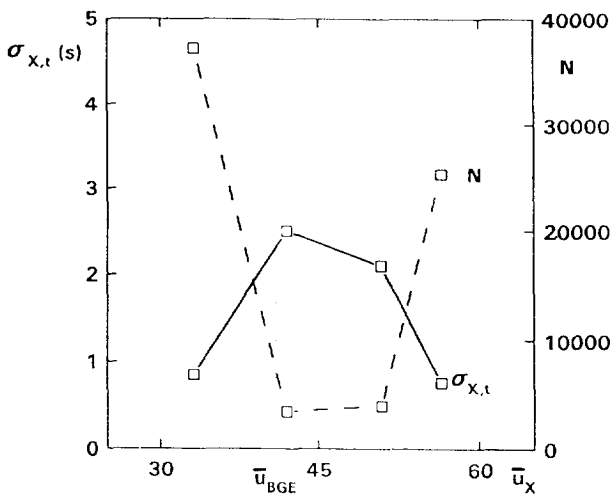

Fig. 11. Experimental verification of the combined effect of front and rear stack expressed as the dependence of the time-based zone width ($\sigma_{X,t}$) and separation efficiency (N) on the mobility of the analytes ($\bar{u}_X$, in 10^{-9} m^2 V^{-1} s^{-1}). Measurements were performed at a constant current of 75 μA in the ITP mode and 100 μA in the CZE step. Leading electrolyte, 10 m*M* HCl–histidine (pH 6.0); terminating electrolyte, 10 m*M* aspartic acid; background electrolyte, 10 m*M* acetic acid–histidine (pH 6.12). The length of the leading segment co-migrating with the sample into the CZE mode was 15 s and the length of the terminating segment was 20 s. Sample, 25 μl of a mixture of $1 \cdot 10^{-6}$ *M* benzoate, iodate, maleate and periodate. The effective mobilities of the analytes at pH 6.12 were calculated from the data given in Table 1. The dotted line corresponds to the splitting point given by the mobility of the BGE co-ion (acetate). Analytes with $\bar{u}_X > \bar{u}_{BGE}$ are controlled by the leading ion as in the T–S–T system, whereas analytes with $\bar{u}_X < \bar{u}_{BGE}$ are controlled by the terminating ion as in the T–S–T system.

dispersion of zones: the first and last zones are the sharpest with the highest separation efficiency and the zones of mobilities very close to the mobility of the co-ion are the most dispersed owing to their early destacking. Comparison with Fig.6 confirms the predicted course of the curves, which can also be expressed in terms of efficiency (see left-hand scale in Fig. 11).

Fig. 12 shows a record of ITP–CZE separation performed in the BGE–S–BGE system where the anomalous zone width distribution is clearly seen, the first and last zones being the sharpest. The lengths of both the leading and terminating segments entering the analytical capillary influence the process of destacking and the migration times of analytes. The longer the segments, the closer the analytes are one to another and the sharper are their zones.

5. Conclusion

In the separation technique combining isotachophoresis and zone electrophoresis on-line, the presence of a segment of leading and/or terminating zones in the CZE stage can never be eliminated. This results in a temporal survival of ITP migration followed by a complicated process of sample destacking, which makes simple rules describing a CZE analysis misleading. The theory presented here describes the destacking process and shows the most important factors affecting this process.

Using a given instrument and electrolyte set-up, the most important factor is the size of the ITP zones cut into the ZE stage. The effects of this factor on the detection time may be characterized in actual systems as follows. In T–S–T systems, the detection times of the analytes increase linearly with increasing amount of leader introduced. In L–S–L systems, the detection time decreases linearly with increasing amount of terminator introduced. These effects relate only to sample zones that are already destacked when passing the detector; to ensure this, the amount of the leader/terminator intro-

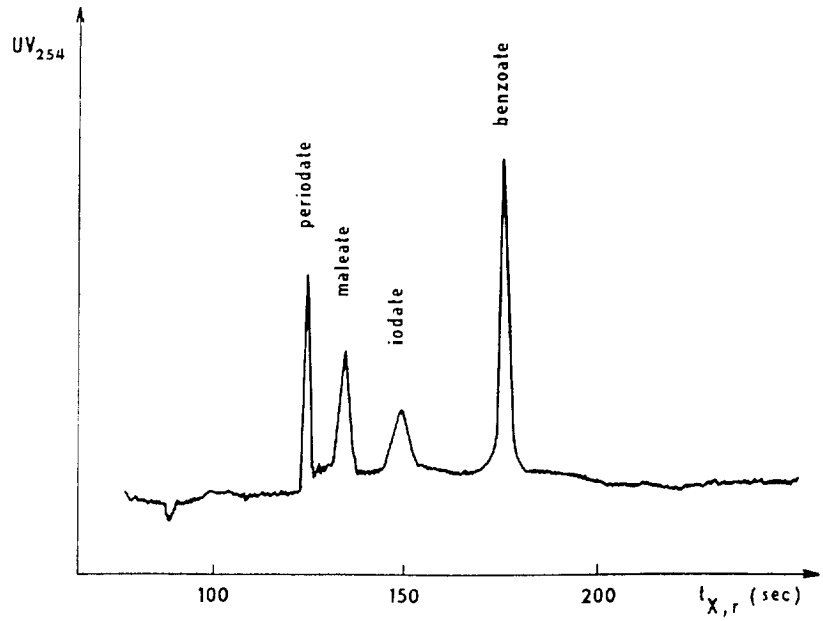

Fig. 12. Effects of destacking process in the BGE–S–BGE system. Experimental conditions as in Fig. 11 except for segment lengths. Leading segment = 15 s, terminator segment = 13 s.

duced must not exceed a certain value that differs from analyte to analyte. The qualitative identification of the analytes based on their variable detection times is possible using a standardization procedure requiring the sample to be run with one internal standard substance.

The temporal stacking also affects the final dispersion of the analyte zones at the point of detection, since the dispersion of zones is frozen as long as they are in stack. The longer the analyte zone remains stacked, the sharper is its peak when detected. The sharpest zones are therefore provided by high-mobility analytes in T–S–T systems and low-mobility analytes in L–S–L systems. BGE–S–BGE systems show an anomalous zone-dispersion distribution, with analytes of intermediate mobilities showing the most dispersed zones.

The theoretical and practical knowledge presented here enables one to formulate some rules for choosing a proper separation mode, electrolyte systems and parameters of the separation with respect to the nature of the sample. T–S–T and L–S–L modes of electrolyte combinations offer simpler operation and evaluation than the BGE–S–BGE system. In the T–S–T system, the slow analytes are destacked first. They are more dispersed but, on the other hand, they are more distant from one another and the risk of stacked migration can be expected to be small. Hence, if the analytes of interest are slow, the T–S–T system may be recommended. If we are interested more in the fast components of the sample and the mobilities of these analytes are very close to the mobility of the leading ion, then it is more convenient to use the L–S–L system where these analytes leave the stack first and the risk of passing the detector still not destacked hardly exists. In both systems, qualitative identification of analytes employing one internal standard is possible on condition that the analytes migrate already fully destacked. The BGE–S–BGE system brings the most uncertainty into the separation and it cannot be recommended unless for a special case. Finally, one can conclude that the simplest to perform, evaluate and optimize seems to be the T–S–T system, in its version where the concentration of T serving as the BGE

is the same as the adjusted concentration of T in the ITP stage.

Acknowledgements

This work was supported by grants from the Grant Agency of the Czech Republic, No. 203/94/0998, and the Grant Agency of the Academy of Sciences of the Czech Republic, No. 431404.

Symbols

D_X	diffusion coefficient of analyte X
i	electric current density
l_j	length of the stacking zone j in the analytical capillary
R	gas constant
T	absolute temperature
t_d	time when the isotachophoretic plateau of the stacking zone in the analytical capillary disappears
$t_{X,e}$	time when substance X leaves the stack
$t_{X,r}$	time when zone X passes through the detector
$t_{z,r}$	time when the sharp boundary of the stacking zone passes through the detector
t_0 (t_L, t_T)	time of migration of the stacking zone into the analytical capillary
u_X	electrophoretic mobility of ion X
$\bar{u}_X$	effective mobility of substance X
v_{T-L}	isotachophoretic velocity in the analytical capillary
v_z	velocity of the sharp boundary of the L–T transition zone
v_{Xj}	migration velocity of analyte X in zone j
x_d	coordinate at which the isotachophoretic plateau of the stacking zone in the analytical capillary disappears
x_r	position of the detector
κ_j	specific conductivity of zone j
$\sigma^2_{X,e}$	variance of zone X when it leaves the stack
$\sigma^2_{X,r}$	detection variance of zone X

References

[1] D. Kaniansky and J. Marák, J. Chromatogr., 498 (1990) 191.
[2] F. Foret, V. Šustáček and P. Boček, J. Microcol. Sep., 2 (1990) 229.
[3] V. Dolník, K.A. Cobb and M. Novotny, J. Microcol. Sep., 2 (1990) 127.
[4] L. Křivánková, F. Foret and P. Boček, J. Chromatogr., 545 (1991) 307.
[5] D.S. Stegehuis, H. Irth, U.R. Tjaden and J. van der Greef, J. Chromatogr., 538 (1991) 393.
[6] F. Foret, E. Szoko and B.L. Karger, J. Chromatogr., 608 (1992) 3.
[7] Ch. Schwer and F. Lottspeich, J. Chromatogr., 623 (1992) 345.
[8] A.P. Tinke, N.J. Reinhoud, W.M.A. Niessen, U.R. Tjaden and J. van der Greef, Rapid Commun. Mass Spectrom., 6 (1992) 560.
[9] D.S. Stegehuis, U.R. Tjaden and J. van der Greef, J. Chromatogr., 591 (1992) 341.
[10] N.J. Reinhoud, A.P. Tinke, U.R. Tjaden, W.M.A. Niessen and J. van der Greef, J. Chromatogr., 627 (1992) 263.
[11] F. Foret, E. Szökö and B.L. Karger, Electrophoresis, 14 (1993) 417.
[12] T.J. Thompson, F. Foret, P. Vouros and B.L. Karger, Anal. Chem., 65 (1993) 900.
[13] T. Hirokawa, A. Ohmori and Y. Kiso, J. Chromatogr., 634 (1993) 101.
[14] N.J. Reinhoud, U.R. Tjaden and J. van der Greef, J. Chromatogr. A, 653 (1993) 303.
[15] N.J. Reinhoud, U.R. Tjaden and J. van der Greef, J. Chromatogr., 641 (1993) 155.
[16] D. Kaniansky, J. Marák, V. Madajová and E. Šimuničová, J. Chromatogr., 638 (1993) 137.
[17] L.M. Benson, A.J. Tomlinson, J.M. Reid, D.L. Walker, M.M. Ames, S. Naylor, J. High Resolut. Chromatogr. 16 (1993) 324.
[18] D. Kaniansky, F. Iványi and F.I. Onuska, Anal. Chem., 66 (1994) 1817.
[19] M. Larsson and S. Någård, J. Microcol. Sep., 6 (1994) 107.
[20] M. Mazereeuw, U.R. Tjaden and J. van der Greef, J. Chromatogr. A, 677 (1994) 151.
[21] S.J. Locke and P. Thibault, Anal. Chem., 66 (1994) 3436.
[22] L. Křivánková, P. Gebauer, W. Thormann, R.A. Mosher and P. Boček, J. Chromatogr., 638 (1993) 119.

[23] P. Boček, M. Deml, P. Gebauer and V. Dolník, Analytical Isotachophoresis, VCH, Weinheim, 1988.
[24] F. Foret, L. Křivánková and P. Boček, Capillary Zone Electrophoresis, VCH, Weinheim, 1993.
[25] L. Křivánková, F. Foret, P. Gebauer and P. Boček, J. Chromatogr., 390 (1987) 3.
[26] V. Šustáček, F. Foret and P. Boček, J. Chromatogr., 545 (1991) 239.
[27] P. Jandik and W.R. Jones, J. Chromatogr., 546 (1991) 431.
[28] H.W. Zhang, X.G. Chen and Z.D. Hu, J. Chromatogr. A, 677 (1994) 159.
[29] P. Gebauer, W. Thormann and P. Boček, J. Chromatogr., 608 (1992) 47.
[30] J. Pospíchal, P. Gebauer and P. Boček, Chem. Rev., 89 (1989) 419.
[31] R. Vespalec, P. Gebauer and P. Boček, Electrophoresis, 13 (1992) 677.